J|A|C|S ARTICLES

Published on Web 04/16/2010

Electrical Contacting of an Assembly of Pseudoazurin and Nitrite Reductase Using DNA-Directed Immobilization

Armand W. J. W. Tepper

Leiden Institute of Chemistry, Leiden University, 2300 RA Leiden, The Netherlands

Received March 1, 2010; E-mail: w.tepper@chem.leidenuniv.nl

Abstract: A method for the electrical contacting of redox enzymes that obtain oxidizing or reducing equivalents from small electron-transfer proteins is demonstrated. The electrochemical contacting of redox enzymes through their immobilization onto electrode supports offers great potential for technological applications and for fundamental studies, but finding appropriate methods to immobilize the enzymes in an orientation allowing rapid electron transfer with the electrode has proven difficult. The copper enzyme nitrite reductase (NiR) and its natural electron-exchange partner pseudoazurin (Paz) are conjugated to a specific DNA tag and immobilized to a gold electrode into a stoichiometrically defined assembly. The DNA tethered to the electrode surface acts as flexible place-holder for the protein components, allowing both proteins to move within the construct. It is shown that Paz efficiently shuttles electrons between the electrode and the NiR enzyme, allowing the electrochemically driven NiR catalysis to be monitored. The activity of the NiR enzyme remains unperturbed by the immobilization. The rate-limiting step of the system is tentatively ascribed to the dissociation of the Paz/NiR complex. The electrochemical response of the system reports not only on the NiR catalysis and on interfacial electron transfer but also on the interaction between NiR and Paz.

Introduction

In this work, DNA-directed immobilization (DDI)[1−6] is employed to electrically contact an enzyme to a macroscopic electrode by immobilizing it together with its natural electron-transfer partner protein into a defined assembly. Establishing an electrical connection between an electrode and a redox enzyme is relevant for technological applications such as biosensing, bioelectronics, biocatalysis, and energy production using biofuel cells.[7] Furthermore, if the electron transfer (ET) between the electrode and a redox enzyme can be made fast enough to out-run the rate of enzyme catalysis, detailed information regarding the mechanisms of enzymatic catalysis and electron transfer can be obtained.[8−11]

Finding methods to immobilize redox enzymes stably and reproducibly and in an orientation allowing rapid electron transfer with an electrode has proven difficult.[7,12] Proteins may lose their native conformation and activity upon physical absorption or chemical coupling to a solid support.[13] A fundamental limitation is related to the exponential decay of the electron-transfer rate with the distance between the donor and acceptor.[14,15] For proteins in which the cofactor is embedded in an electrically insulating protein matrix, the cofactor of the enzyme has to be within approximately 1.8 nm of the electrode to yield ET rates exceeding 100/s,[14,15] the latter rate corresponding to the turnover rate of a typical enzyme. For some proteins, especially large enzymes carrying deeply buried cofactors, this can be difficult or even impossible to achieve. A number of strategies have been devised to mitigate these problems, including protein "hot-wiring",[7,12,16,17] embedding the proteins in redox-active polymer matrices,[18,19] the use of (co-immobilized) redox mediators,[4,20,21] the creation of protein chimeras,[22] the fusion of proteins with nanoparticles,[23−26] and the use of heterogeneous electrode matrices such as pyrolytic

(1) Fruk, L.; Muller, J.; Weber, G.; Narvaez, A.; Dominguez, E.; Niemeyer, C. M. *Chemistry* **2007**, *13* (18), 5223–5231.
(2) Niemeyer, C. M. *Biochem. Soc. Trans.* **2004**, *32* (Pt 1), 51–53.
(3) Muller, J.; Niemeyer, C. M. *Biochem. Biophys. Res. Commun.* **2008**, *377* (1), 62–67.
(4) Piperberg, G.; Wilner, O. I.; Yehezkeli, O.; Tel-Vered, R.; Willner, I. *J. Am. Chem. Soc.* **2009**, *131* (25), 8724–8725.
(5) Mirkin, C. A.; Letsinger, R. L.; Mucic, R. C.; Storhoff, J. J. *Nature* **1996**, *382* (6592), 607–609.
(6) Mirkin, C. A. *Inorg. Chem.* **2000**, *39* (11), 2258–2272.
(7) Willner, B.; Katz, E.; Willner, I. *Curr. Opin. Biotechnol.* **2006**, *17* (6), 589–596.
(8) Armstrong, F. A. *Curr. Opin. Chem. Biol.* **2005**, *9* (2), 110–117.
(9) Heering, H. A.; Wiertz, F. G.; Dekker, C.; de Vries, S. *J. Am. Chem. Soc.* **2004**, *126* (35), 11103–11112.
(10) Hirst, J. *Biochim. Biophys. Acta* **2006**, *1757* (4), 225–239.
(11) Wijma, H. J.; Jeuken, L. J.; Verbeet, M. P.; Armstrong, F. A.; Canters, G. W. *J. Am. Chem. Soc.* **2007**, *129* (27), 8557–8565.
(12) Heering, H. A.; Canters, G. W. Activating Redox Enzymes through Immobilisation and Wiring. In *Engineering the Bioelectronic Interface: Applications to Analyte Biosensing and Protein Detection*; Davis, J. J., Ed.; Royal Society of Chemistry: Cambridge, 2010; pp 120−153.
(13) Rusmini, F.; Zhong, Z.; Feijen, J. *Biomacromolecules.* **2007**, *8* (6), 1775–1789.
(14) Williams, R. J. *Biochem. Soc. Trans.* **2005**, *33* (Pt 4), 825–828.
(15) Gray, H. B.; Winkler, J. R. *Q. Rev. Biophys.* **2003**, *36* (3), 341–372.
(16) Bardea, A.; Katz, E.; Buckmann, A. F.; Willner, I. *J. Am. Chem. Soc.* **1997**, *119* (39), 9114–9119.
(17) Zayats, M.; Katz, E.; Willner, I. *J. Am. Chem. Soc.* **2002**, *124* (49), 14724–14735.
(18) Aoki, A.; Heller, A. *J. Phys. Chem.* **1993**, *97* (42), 11014–11019.
(19) Rajagopalan, R.; Aoki, A.; Heller, A. *J. Phys. Chem.* **1996**, *100* (9), 3719–3727.
(20) Astier, Y.; Canters, G. W.; Davis, J. J.; Hill, H. A.; Verbeet, M. P.; Wijma, H. J. *ChemPhysChem* **2005**, *6* (6), 1114–1120.
(21) Liu, Y.; Wang, M. K.; Zhao, F.; Liu, B. F.; Dong, S. J. *Chem.—Eur. J.* **2005**, *11* (17), 4970–4974.
(22) Dodhia, V. R.; Fantuzzi, A.; Gilardi, G. *J. Biol. Inorg. Chem.* **2006**, *11* (7), 903–916.

10.1021/ja101515y

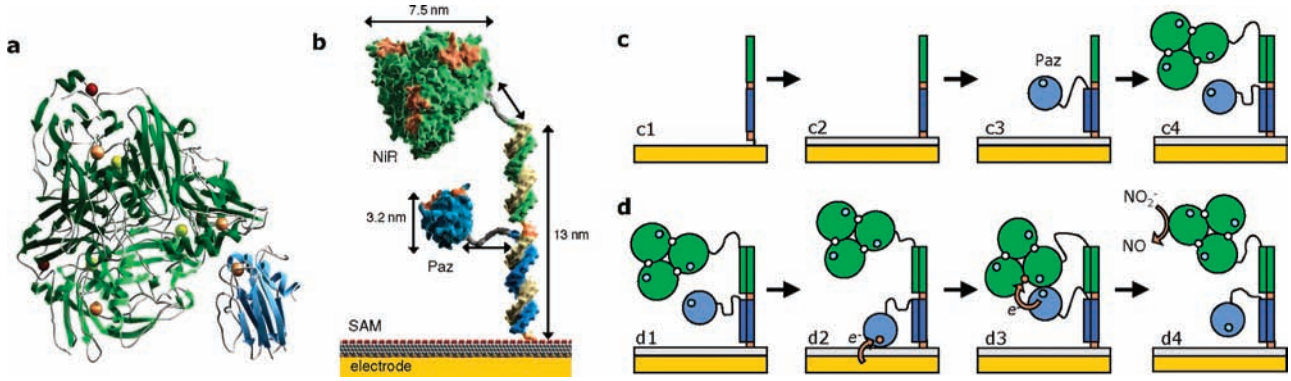

Figure 1. (a) Electron-transfer complex between trimeric copper NiR (green) and Paz (blue), both from *Alcaligenis feacalis*.[31] Spheres indicate the NiR and Paz type-1 copper sites involved in electron transfer (orange), the NiR type-2 copper involved in the binding and conversion of substrate (yellow), and the N-terminus (dark red). (b) An atomic 3D model illustrating the approximate dimensions of the construct. The electron-transfer patches on NiR and Paz are shown in orange. Although the structure is shown with the DNA "standing-up", it is expected that the anchor can bend and rotate around the nonpairing thymine residues of the anchor (orange). (c) Device assembly, showing the binding of the anchor SH-DNA (c1), backfilling with a SAM of an organic thiol (c2), and the hybridization of Paz-L-DNA_{TP} (c3) and of NiR-L-DNA_{TN} (c4). Small spheres indicate the copper cofactors. (d) Simplified envisaged mechanism. The cycle starts with all proteins in the oxidized form (d1). Paz moves to the surface and takes up an electron (d2). The NiR-Paz ET complex forms, and the electron is transferred from Paz to the NiR type-1 Cu site (d3) and then to the type-2 copper where it is used to reduce nitrite (d4), completing the cycle. Although the ET process is shown between Paz and NiR on a single anchor chain, a NiR molecule on one anchor strand may also be supplied with electrons by a Paz molecule on a neighboring strand, provided the constructs are close enough (see text for details).

graphite.[8,10,27] In nearly all of these strategies, the protein is statically immobilized on the electrode surface. On the other hand, small and stable electron-transfer proteins (e.g., cyt *c*, cupredoxins) carrying a cofactor nearby the protein's surface often interface well with electrodes, and many of them have been studied using electrochemical methods (e.g., refs 9, 15, 27−30).

In nature, the kinetic electron-transfer barrier is overcome by creating short distances between the donor and the acceptor, for example by the formation of specific ET complexes between two partner proteins. An example is the complex between pseudoazurin (Paz) and copper nitrite reductase (NiR), the two proteins utilized in this study. To sustain high turnover rates, such ET complexes are often "transient" in the sense that they are characterized by fast association and dissociation rates (k_{off} > 500/s for the Paz/NiR complex).[31,32] The nitrite reductases have a crucial function in denitrification by catalyzing the one-electron reduction of nitrite to nitric oxide. Each monomer of the homotrimeric NiR (111 kDa) from *Alcaligenes faecalis* contains one type-1 ("blue") copper and a type-2 copper center, whereas Paz (14 kDa) from the same organism contains a single type-1 copper cofactor. Both proteins and their complex have been extensively characterized on structural and mechanistic levels (e.g., refs 11, 20, 31−36). The NiR enzyme has also been absorbed to pyrolytic graphite and studied electrochemically.[11] The biological relevance, the significant body of experimental information available, and the prospect of using electrically contacted NiR to provide a specific NO_2^-/NO biosensor make this system an appropriate model to test the viability of the method proposed in this study.

Instead of relying on a direct contact of the enzyme with the electrode, the presented method proposes the use of DDI to connect the enzyme (i.e., NiR) together with its electron-transfer partner protein (i.e., Paz) in a stoichiometrically defined assembly to a gold electrode surface (Figure 1). It is expected that both proteins retain a degree of mobility in the construct, allowing Paz to reach the electrode surface in an orientation suitable for ET, while subsequently providing the translational and rotational freedom for Paz and Nir to form their characteristic ET complex. In contrast to NiR, its electron-transfer partner Paz interfaces well with modified Au electrode surfaces and is envisioned to shuttle electrons between the electrode and the enzyme to drive the catalytic turnover.

The assembly and an electrochemical characterization of the Paz/NiR construct are presented. The experimental data are consistent with the envisioned mechanism. Cyclic voltammetry (CV) is used to evaluate the electrochemical response in terms of electron-transfer kinetics. The catalysis is studied as a function of the nitrite substrate concentration and compared to data obtained for the isolated wild-type enzyme. The ionic strength dependence of the catalytic output current reveals the importance of electrostatic interactions between the components in the construct and indicates that the rate-limiting step is associated with the Paz/NiR interaction. The electrochemistry of the system

(23) Katz, E.; Willner, I. *Angew. Chem., Int. Ed.* **2004**, *43* (45), 6042–6108.
(24) Yehezkeli, O.; Yan, Y. M.; Baravik, I.; Tel-Vered, R.; Willner, I. *Chem.—Eur. J.* **2009**, *15* (11), 2674–2679.
(25) Yan, Y. M.; Yehezkeli, O.; Willner, I. *Chem.—Eur. J.* **2007**, *13* (36), 10168–10175.
(26) Xiao, Y.; Patolsky, F.; Katz, E.; Hainfeld, J. F.; Willner, I. *Science* **2003**, *299* (5614), 1877–1881.
(27) Hagen, W. R. *Eur. J. Biochem.* **1989**, *182* (3), 523–530.
(28) Baymann, F.; Barlow, N. L.; Aubert, C.; Schoepp-Cothenet, B.; Leroy, G.; Armstrong, F. A. *FEBS Lett.* **2003**, *539* (1−3), 91–94.
(29) Davis, J. J.; Burgess, H.; Zauner, G.; Kuznetsova, S.; Salverda, J.; Aartsma, T.; Canters, G. W. *J. Phys. Chem. B* **2006**, *110* (41), 20649–20654.
(30) Marshall, N. M.; Garner, D. K.; Wilson, T. D.; Gao, Y. G.; Robinson, H.; Nilges, M. J.; Lu, Y. *Nature* **2009**, *462* (7269), 113–116.
(31) Impagliazzo, A.; Blok, A. J.; Cliff, M. J.; Ladbury, J. E.; Ubbink, M. *J. Am. Chem. Soc.* **2007**, *129* (1), 226–233.
(32) Wijma, H. J. Catalytic mechanism and protein engineering of copper-containing nitrite reductase. PhD thesis, Leiden Univeristy, The Netherlands, 2006.
(33) Vlasie, M. D.; Fernandez-Busnadiego, R.; Prudencio, M.; Ubbink, M. *J. Mol. Biol.* **2008**, *375* (5), 1405–1415.
(34) Wijma, H. J.; Canters, G. W.; de Vries, S.; Verbeet, M. P. *Biochemistry* **2004**, *43* (32), 10467–10474.
(35) Wijma, H. J.; Jeuken, L. J.; Verbeet, M. P.; Armstrong, F. A.; Canters, G. W. *J. Biol. Chem.* **2006**, *281* (24), 16340–16346.
(36) Astier, Y.; Bond, A. M.; Wijma, H. J.; Canters, G. W.; Hill, H. A. O.; Davis, J. J. *Electroanalysis* **2004**, *16* (13−14), 1155–1165.

Table 1. Composition and DNA Sequences of the Conjugates Used in This Study[a]

Component	Composition and sequence
SH-DNA$_{PN}$	5' HS-C_6-TACTCTAAGGTGACGATGATTGGCTGGCGGAAGGTGAGA 3'
SH-DNA$_{NP}$	5' HS-C_6-TGGCTGGCGGAAGGTGAGATTACTCTAAGGTGACGATGA 3'
SH-DNA$_{P}$	5' HS-C_6-ACTCTAAGGTGACGATGA 3'
SH-DNA$_{N}$	5' HS-C_6-GGCTGGCGGAAGGTGAGA 3'
Paz-L-DNA$_{TP}$	5' Paz-NH-PEO_5-C_6-TCATCGTCACCTTAGAGT 3'
NiR-L-DNA$_{TN}$	5' NiR-NH-PEO_5-C_6-TCTCACCTTCCGCCAGCC 3'

[a] Sequences for the hybridization of Paz or NiR are colored blue and green, respectively. Nonpairing "hinge" residues are colored orange. The subscripts P, N, and T refer to Paz, NiR, and Tag, respectively.

is studied as a function of the density of anchor DNA on the surface. The relevance of the findings toward the electrical contacting of redox enzymes and the study of protein−protein interactions is discussed.

Materials and Methods

Oligos and Conjugate Synthesis. Modified HPLC-purified oligos were obtained from Isogen Lifescience, NL. The anchor SH-DNAs were obtained in the trityl protected form and deprotected employing $AgNO_3$ and DTT according to the manufacturer supplied protocol. NH_2-C_6-DNA$_{TP}$ and NH_2-C_6-DNA$_{TN}$ were coupled to the N-terminus of Paz and NiR, respectively, using a bifunctional NHS (NHS = *N*-succinimidyl ester) PEO linker, bis(NHS)$(PEO)_5$ (Pierce). Briefly, 1 mM protein and 1 mM NH_2-C_6-DNA were incubated with a 2-fold excess of the linker at pH 7.5 and at room temperature, typically for 2 h. Excess DNA and linker were then removed from the reaction mixture employing Superdex 30 (GE Healthcare) gel-filtration chromatography (0.1 M P_i, pH 6.8). The ionic strength of the fractions containing the desired product and uncoupled protein was lowered by diluting the sample 10-fold with water, after which the solution was applied to 1 mL anion exchange sepharose-Q column (GE Heathcare). The desired product was eluted from the column as a single peak employing a 15 min linear gradient of 0−0.75 M NaCl in 20 mM P_i, pH 6.8. The identity of the product was confirmed utilizing the characteristic optical absorptions of DNA (DNA$_{TP}$, $\varepsilon_{260nm} = 152$ mM^{-1} cm^{-1}; DNA$_{TN}$, $\varepsilon_{260nm} = 134$ mM^{-1} cm^{-1}) and the UV absorptions of Paz ($\varepsilon_{280nm} = 5.7$ mM^{-1} cm^{-1}) and NiR ($\varepsilon_{280nm} = 46$ mM^{-1} cm^{-1}), as well as the absorptions of the oxidized copper cofactors of Paz ($\varepsilon_{594nm} = 2.9$ mM^{-1} cm^{-1}) or NiR ($\varepsilon_{460nm} = 2.9$ mM^{-1} cm^{-1}).

Electrode Preparation and Assembly. Gold electrodes of 0.031 cm^2 surface area (CH instruments, USA) were subsequently polished with 1, 0.3, and 0.05 μm aluminum oxide (Buehler, Düsseldorf, Germany) on a polishing cloth and sonicated for 1 min in ultrapure water. The SH-DNA anchor was then deposited on the Au by immersing the electrode in a 1 μM solution of the anchor DNA (in 0.1 M P_i, 1 M NaCl, pH 6.8) for a given period (the "seeding time") varying between 5 s and 30 min, followed by rinsing with 0.5 M P_i at pH 6.8. The SH-DNA containing electrodes were then exposed to a solution of 1 mM 1-mercaptohexanol (MHX) in 0.5 M P_i, pH 6.8, for at least 1 h and then extensively rinsed with water. The Paz-L-DNA$_{TP}$ and/or NiR-L-DNA$_{TN}$ were subsequently hybridized to the anchor DNA from 0.1−0.3 μM solutions of either construct in 0.20 M P_i, pH 6.8, typically for 1 h, followed by rinsing with buffer. In most cases the hybridization was followed by cyclic voltammetry as illustrated in Figure 3b.

Cyclic Voltammetry. All measurements were carried out in the apparatus schematically depicted in Figure S6 in Supporting Information. It contained the Au working electrode immersed in a small drop of anaerobic buffer solution (15−75 μL) in contact with a calomel reference electrode (0.241 V vs NHE) and a platinum wire counter electrode. The setup was surrounded by an Ar atmosphere and controlled by a μ-lab potentiostat (Ecochemie, The Netherlands). The scan rate was 10 mV/s with a 1 mV step potential unless stated otherwise. The ionic strength of the solution was varied by changing the concentration of the phosphate buffer. For the experiments involving NO, the NO gas was generated directly in the airtight electrode chamber by acid hydrolysis of 5 mg of spermine NONOate by at pH 4, providing an atmosphere of ∼1.5% NO, corresponding to ∼4 μM NO in solution.

DNA Quantification. The density of DNA on electrode surfaces was quantified using redox-active ruthenium(III) hexamine (RuHex).[37−40] RuHex binds stoichiometrically to the DNA phosphate backbone groups and can be assayed using cyclic voltammetry. Briefly, DNA-seeded and MHX-backfilled electrodes were incubated with 5 μM RuHex in 10 mM argon-purged Tris buffer (pH 7.4) for at least 20 min at room temperature. Voltammograms were then recorded under anaerobic conditions in the same solution in the voltage range of 0.24 to −0.30 V versus NHE using a scan-rate of 0.5 V/s. After the subtraction of the capacitive background, the quantity of RuHex bound to the phosphate groups of the DNA backbone was determined by integrating the cathodic peak and using the relation $\Gamma_{Ru} = Q/nFA$ where Q is the integrated charge, n is the number of electrons in the redox reaction, F is the Faraday constant (in C/mol), and A the electrode area (in cm^2). The quantity of DNA on the surface, Γ_{DNA}, was then calculated from Γ_{Ru} using $\Gamma_{DNA} = \Gamma_{Ru}(z/m)N_A$ where m is the number of nucleotides in the DNA strand, z the charge of the redox molecules, and N_A is Avogadro's number. Since the treatment with RuHex rendered the electrodes unsuitable for the hybridization of the Paz and NiR constructs, the density of anchor DNA on freshly prepared electrodes was estimated from the seeding time using binding isotherms (Figure S1 in Supporting Information).

Results and Discussion

Design of the Construct. The construct characterized in this work is schematically depicted in Figure 1. Paz and NiR are both conjugated to a specific 18-bp ssDNA oligonucleotide tag using a 22 Å long hydrophilic bis(NHS)$(PEO)_5$ linker (Table 1). The DNA tags contain a 8 Å long C_6-NH_2 linker at the 5′ terminus to facilitate the coupling, thus providing a total length of the spacer arm of 3 nm. The N-terminus, i.e., the preferred attachment point of the PEO linker on the protein, occurs far from the Paz/NiR interaction interface (colored orange in Figure 1a). It is thus expected that the immobilization does not interfere with the molecular recognition between Paz and NiR. The DNA tags direct the proteins to a single-stranded SH-DNA anchor strand tethered to the gold electrode surface through a stable thiol linkage. To increase the flexibility of the construct, the anchors SH-DNA$_{PN}$ and SH-DNA$_{NP}$ contain two nonpairing

(37) Steel, A. B.; Herne, T. M.; Tarlov, M. *J. Anal. Chem.* **1998**, *70* (22), 4670–4677.
(38) Steel, A. B.; Levicky, R. L.; Herne, T. M.; Tarlov, M. J. *Biophys. J.* **2000**, *79* (2), 975–981.
(39) Su, L.; Sankar, C. G.; Sen, D.; Yu, H. Z. *Anal. Chem.* **2004**, *76* (19), 5953–5959.
(40) Yu, H. Z.; Luo, C. Y.; Sankar, C. G.; Sen, D. *Anal. Chem.* **2003**, *75* (15), 3902–3907.

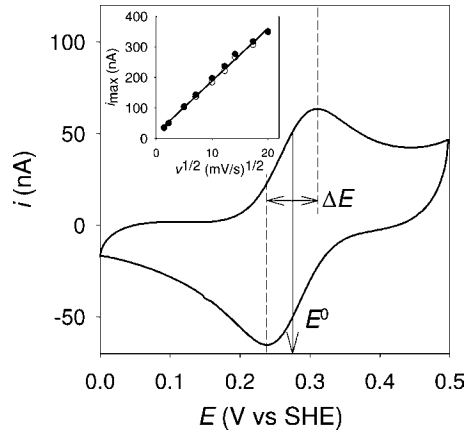

Figure 2. Cyclic voltammetry of 20 μM pseudoazurin in solution (5 mV/s, 0.1 M P_i, pH 6.8) on MHX modified gold. The inset shows the linear dependence of the peak current (i_{max}) in both scan directions (solid and open circles, respectively) on the square root of the scan rate ($v^{1/2}$).

thymine residues in between the regions complementary to the tags on the Paz and NiR conjugates, as well as one nonpairing thymine at its base (orange in Figure 1).

SAM Selection and Cyclic Voltammetry of Paz in Solution. The direct binding of proteins to bare gold may cause protein denaturation and consequent loss of function.[41−43] To shield the protein from the gold, the surface can be modified with a self-assembled monolayer (SAM) of an organic thiol yielding a regular, tunable, and more biocompatible surface.[44] For the current purpose, it was necessary to select a SAM that allowed rapid ET from the electrode to the Paz protein, while minimizing the absorption of Paz to the surface. These requirements were met by a SAM of 1-mercapto-6-hexanol (MHX), as shown by cyclic voltammetry (CV) of freely diffusing Paz in solution (Figure 2). The voltammograms are characterized by a midpoint potential (E^0) of 275 mV, comparing well with the E^0 values between 260 and 280 mV reported in the literature.[36] The peak-to-peak separation ΔE is 61 mV at low scan rates, the latter being close to the ideal value of 59 mV for a freely diffusing (nonabsorbed) redox-active species. The peak current (i_{max}) was equal in both scan directions and varied linear with the square root of the scan rate ($v^{1/2}$) up to at least 500 mV/s (Figure 2, inset), demonstrating electrochemical reversibility. Conversely, the NiR enzyme in solution did not show a response on MHX-modified Au electrodes, neither in the presence nor in the absence of 1 mM of the nitrite substrate.

MHX has been used extensively as a backfilling agent of gold seeded with thiolated DNAs (e.g., refs 37, 38, 45, 46). The physical properties of DNA/MHX films as well as the kinetics of hybridization of complementary sequences have been characterized by a wide variety of methods, including atomic force,[47] neutron reflectivity,[48] fluorescence,[49] and surface plasmon resonance[50] spectroscopies. These studies showed that the MHX removes unspecifically absorbed ssDNA and that it makes the specifically chemisorbed DNA available for hybridization.[45]

Hybridization Efficiency. To check whether the Paz and NiR constructs were capable of hybridizing to the anchor strand and to estimate the binding stoichiometry, the DNA bound to the surface of identically treated, MHX-backfilled electrodes containing (1) only SH-DNA_{PN}, (2) SH-DNA_{PN} + Paz-L-DNA_{TP}, or (3) SH-DNA_{PN} + Paz-L-DNA_{TP} + NiR-L-DNA_{TN} was quantified using CV of ruthenium hexamine (RuHex; see Materials and Methods). The DNA density (20 s of incubation with SH-L-DNA_{PN}) for case 1 was determined at 1.3×10^{12} molecules/cm^2. The integrated current of the RuHex peak, which is proportional to the number of DNA backbone phosphate groups on the surface, normalized to that measured for the electrode containing only the anchor varied according to 1.0:1.4:2.5 for cases 1, 2 and 3, respectively. Renormalization to the number of phosphates per anchor molecule expected in each case (39, 57, and 75 for cases 1, 2, and 3, respectively) yielded a binding stoichiometry of 1.0:1.0:1.3 with an estimated error of 0.2, thus indicating a near 100% hybridization efficiency for both the Paz-L-DNA_{TP} and NiR-L-DNA_{TN} constructs at this density of anchor DNA.

Catalytic Activity and Controls. Electrodes were assembled according to the procedure in Figure 1c. Figure 3a displays cyclic voltammograms recorded using an Au electrode seeded with $2.0 \pm 0.3 \times 10^{12}$ molecules/cm^2 anchor DNA, backfilled with MHX, and hybridized with the Paz-L-DNA_{TP} and Nir-L-DNA_{TN} constructs. A reversible quasi-sigmoidal response typical for surface-associated catalysis[8,10] was reproducibly detected in the presence of the nitrite substrate but not in its absence. Rinsing the electrode or storing it for 24 h at 4 °C (covering the electrode with a small drop of buffer) did not alter the response, showing that the enzyme constructs were tightly associated with the electrode surface. The catalytic response was not observed using identically treated electrodes but with one of the four principal components (either anchor SH-DNA_{PN}, Paz-L-DNA_{TP}, NiR-L-DNA_{TN}, or the MHX SAM) left out, thus showing that all components were required for catalytic activity and suggesting that the system operates according to the mechanism in Figure 1d. Negligible catalysis was observed with electrodes containing only the Paz-L-DNA_{TP} component and up to 10 μM wild-type NiR in solution, showing that the spatial proximity of Paz and NiR is required for catalysis. Furthermore, the addition of the DNA hydrolyzing enzyme DNase I to the solution to the electrode solution led to a time-dependent decrease in the amplitude of i_{cat} (Figure S2 in Supporting Information), consistent with the destruction of the DNA linking the proteins to the surface. The kinetics of the assembly process could be conveniently followed by CV (Figure 3b). In typical cases, the amplitude of the catalytic current (i_{cat}) increased with a rate constant in the order of 5 h^{-1} after the addition of 0.2 μM of the NiR construct to the solution on top of electrodes preassembled with the Paz construct. The process occurs on a time scale compatible with the hybridization of DNA on surfaces under conditions similar to those employed here.[46,51,52]

(41) Davis, J. J.; Hill, H. A. O. *Chem. Commun.* **2002**, (5), 393–401.
(42) Terrettaz, S.; Ulrich, W. P.; Vogel, H.; Hong, Q.; Dover, L. G.; Lakey, J. H. *Protein Sci.* **2002**, *11* (8), 1917–1925.
(43) Ferrero, V. E. V.; Andolfi, L.; Di Nardo, G.; Sadeghi, S. J.; Fantuzzi, A.; Cannistraro, S.; Gilardi, G. *Anal. Chem.* **2008**, *80* (22), 8438–8446.
(44) Love, J. C.; Estroff, L. A.; Kriebel, J. K.; Nuzzo, R. G.; Whitesides, G. M. *Chem. Rev.* **2005**, *105* (4), 1103–1170.
(45) Arinaga, K.; Rant, U.; Tornow, M.; Fujita, S.; Abstreiter, G.; Yokoyama, N. *Langmuir* **2006**, *22* (13), 5560–5562.
(46) Gao, Y.; Wolf, L. K.; Georgiadis, R. M. *Nucleic Acids Res.* **2006**, *34* (11), 3370–3377.
(47) Erts, D.; Polyakov, B.; Olin, H.; Tuite, E. *J. Phys. Chem. B* **2003**, *107* (15), 3591–3597.
(48) Levicky, R.; Herne, T. M.; Tarlov, M. J.; Satija, S. K. *J. Am. Chem. Soc.* **1998**, *120* (38), 9787–9792.
(49) Murphy, J. N.; Cheng, A. K. H.; Yu, H. Z.; Bizzotto, D. *J. Am. Chem. Soc.* **2009**, *131* (11), 4042–4050.
(50) Georgiadis, R.; Peterlinz, K. P.; Peterson, A. W. *J. Am. Chem. Soc.* **2000**, *122* (13), 3166–3173.

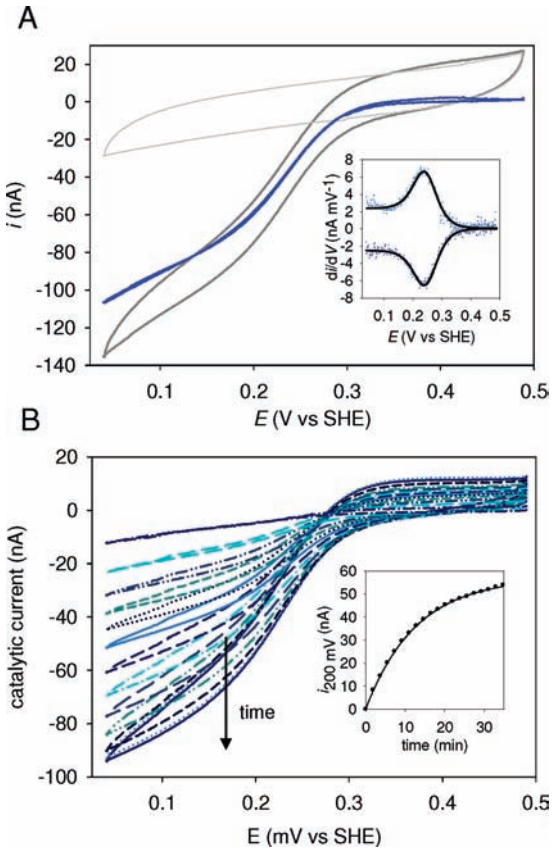

Figure 3. (a) Cyclic voltammetry of a fully assembled electrode in the presence (dark gray) and in the absence (light gray) of 1 mM NO_2^-, as well as the difference (blue) recorded at 5 mV/s. Inset: first derivatives of the traces in both scan directions (points) fit to eq 2 (black lines). (b) Background corrected voltammograms recorded at 10 mV/s showing the increase of the amplitude of the catalytic signal in time after the addition of 0.3 μM NiR-L-DNA_{TN} to an electrode containing anchor SH-DNA_{PN}, MHX, and Paz-L-DNA_{TP} (0.20 M P_i, pH 6.8, 1 mM NO_2^-). The time difference between each subsequent voltammogram is 108 s. The inset shows the catalytic current at 200 mV as a function of the incubation time. The solid line is a fit to a monoexponential decay function with $k = 5\ h^{-1}$.

Reversible catalysis was also observed using the "reverse" anchor SH-DNA_{NP} where Paz-L-DNA_{TP} and NiR-L-DNA_{TN} are in the opposite configuration on the anchor strand (i.e., with NiR closest to the electrode) (Figure S3 in Supporting Information). Also in this configuration the Paz-L-DNA_{TP} component was required for the catalytic signal to appear, thus showing that NiR does not communicate with the electrode, even if it is brought in close proximity to the electrode, and confirming that Paz acts as an electron shuttle. The detection of catalysis in the opposite configuration illustrates the flexibility of the construct, possibly involving bending and/or rotation around the nonpairing thymine residues on the anchor.

Electrode Response versus [NO_2^-] and the Detection of NO. To check the functional integrity of the immobilized construct, the dependence of the catalytic current on [NO_2^-] was studied. The catalytic mechanism of NiR from *A. faecalis* involves two parallel pathways characterized by a random order of nitrite binding and T2 copper site reduction (Scheme S1 in Supporting Information). Consequently, the enzyme does not follow standard Michaelis−Menten kinetics. Instead, the expression relating the steady-state rate of substrate turnover (which is proportional to the measured current) with the [NO_2^-] is given by:[32,35]

$$i_t = i_{cat}^A[NO_2^-]\frac{1 + \frac{k_{cat}^B}{k_{cat}^A}\frac{[NO_2^-]}{K_M^B}}{K_M^A + [NO_2^-] + \frac{[NO_2^-]2}{K_M^B}} \quad (1)$$

where i_t is the observed catalytic current of the NiR at given potential, i_{cat}^A is the catalytic current due to catalysis by the "upper" route (see Scheme S1 in Supporting Information), K_M^A and K_M^B are the Michaelis constants for nitrite binding to the "upper" and "lower" route, respectively, and k_{cat}^A and k_{cat}^B are the corresponding rate constants. Cyclic voltammograms using a fully assembled electrode ($2.2 \pm 0.3 \times 10^{12}$ anchors/cm^2) were recorded at various [NO_2^-]. The catalytic current was measured at 180 mV (where the effects of mass transport and the reductive inactivation of NiR[11] are minimal) and plotted against [NO_2^-] as shown in Figure 4a. The data are well fit by eq 1, yielding kinetic parameters ($K_M^A = 28 \pm 6\ \mu M$, $K_M^B = 1.1 \pm 0.2$ mM, and $k_{cat}^B/k_{cat}^A = 2.7 \pm 0.2$) comparable to literature values measured under similar conditions.[32,35] Furthermore, in Figure 4b it is shown that the system can detect the oxidation of NO at pH 8.6 as shown earlier for isolated NiR.[34] The catalytic wave is centered at $E_M = 240$ mV, which is within the experimental error of the E_M observed for nitrite turnover (see below). The observations confirm that the electrochemical response of

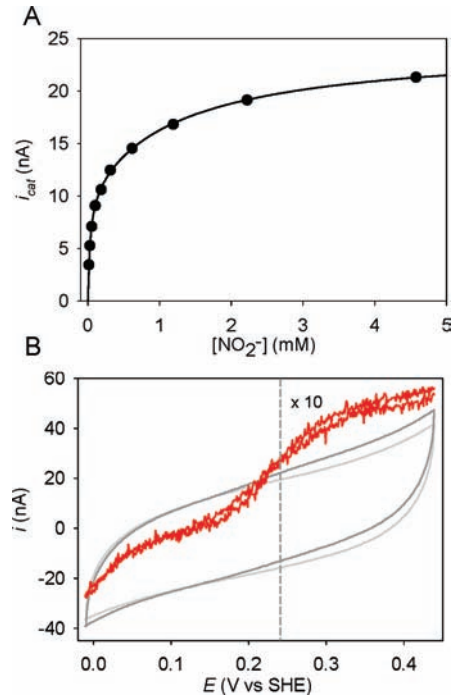

Figure 4. (a) Catalytic current measured at 180 mV against [NO_2^-] using an electrode seeded with SH-DNA_{PN} ($2.2 \pm 0.3 \times 10^{12}$ anchors/cm^2) and assembled with Paz-L-DNA_{TP} and NiR-L-DNA_{TN}. The data were fit using eq 1 derived for the catalytic mechanism of NiR (see text for details). (b) NO oxidase activity of the construct at pH 8.6 in 0.1 M HEPES. The difference (red) between the cyclic voltammograms in the absence (light gray) and presence (dark gray) of ~4 μM NO reveals a catalytic wave centered around 240 mV. The negative current at $E < 0.1$ V is due to oxygen leakage into the system during the experiment.

(51) Peterson, A. W.; Heaton, R. J.; Georgiadis, R. M. *Nucleic Acids Res.* **2001**, *29* (24), 5163–5168.
(52) Peterlinz, K. A.; Georgiadis, R. M.; Herne, T. M.; Tarlov, M. J. *J. Am. Chem. Soc.* **1997**, *119* (14), 3401–3402.

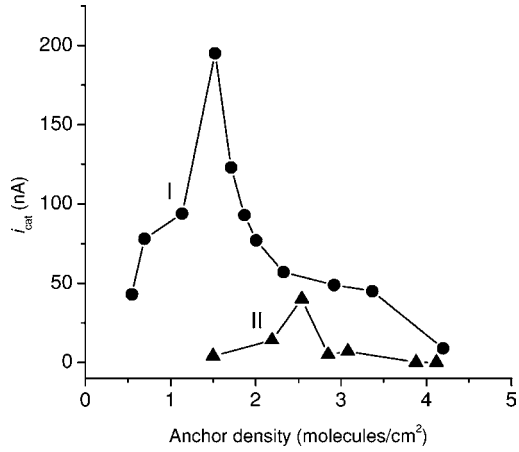

Figure 5. Catalytic current measured at 0 V versus SHE employing 1 mM nitrite in 0.2 M P_i buffer, pH 6.8, as a function of the density of the anchor on the surface using the full length anchor SH-DNA_{PN} (●) or a 1:1 mix of the SH-DNA_P + SH-DNA_N anchors (▲).

assembled electrodes reflect substrate turnover by the NiR enzyme and that the DNA immobilization did not perturb the catalytic properties of NiR.

Dependence of the Catalytic Current on the Surface Density of Anchor DNA. The dynamic nature of the proposed mechanism suggests that a construct needs space on the electrode to operate. To study this in some detail, the electrochemical response was studied as a function of the density of anchor DNA on the surface as measured using RuHex. Electrodes containing different densities of anchor SH-DNA_{PN} were prepared, backfilled with MHX, hybridized with Paz-L-DNA_{TP} and NiR-L-DNA_{TN}, and assayed for catalytic activity employing 1 mM NO_2^- in 0.2 M P_i, pH 6.8 using CV. Figure 5 shows i_{cat} measured at 0 V versus anchor DNA density. After an initial increase of i_{cat} with density, a maximum is reached at 1.5×10^{12} anchors/cm^2, after which i_{cat} drops off steeply. The initial increase in i_{cat} versus density can be explained by the increasing amount of enzyme on the surface. The progressive decrease in i_{cat} at densities higher than 1.5×10^{12} molecules/cm^2 can be rationalized by assuming that Paz is hindered from reaching the electrode surface as a result of steric hindrance by neighboring assemblies and/or that the hybridization of the Paz and NiR constructs becomes less efficient. For a 25 bp DNA immobilized on a gold surface it has been shown that the hybridization efficiency with the complementary ssDNA steeply drops off at DNA densities higher than 4×10^{12} molecules/cm^2.[37] In the current case this drop-off might occur at lower densities because the anchor is longer (39 bases), while it has to hybridize two oligonucleotides that are each conjugated to a bulky protein.

At the optimum density of 1.5×10^{12} anchors/cm^2, the constructs are spaced at an average distance of 8.2 nm (assuming a homogeneous distribution of molecules on the surface), which is smaller than the approximate dimensions of the construct on the surface (see Figure 1b). It is conceivable, therefore, that a NiR molecule on one anchor strand is supplied with electrons by a Paz molecule on a neighboring strand. To evaluate whether such a mechanism could occur, electrodes with varying densities of a 1:1 mix of Paz and NiR anchor molecules (SH-DNA_P and SH-DNA_N, see Table 1) were prepared, hybridized with Paz-L-DNA_{TP} and NiR-L-DNA_{TN}, and assayed for catalytic activity. The observed currents were much lower than in the case of electrodes prepared using the full-length anchor SH-DNA_{PN}. Part of this difference is due to the fact that the density of the proteins is higher and that the number of interactions is larger in the case of the full length construct when both proteins are present on a single anchor strand. For example, assuming that each construct is surrounded by six neighbors within the appropriate distance for ET, the number of interactions is six for the full-length construct and three, on average, in the mixed-anchor case. This, combined with the 2-fold higher density of proteins in the full-length construct could account for a 4-fold higher current generated by the "through neighbor" pathway for the full-length construct with respect to the mixed-anchor case. Thus, the "through neighbor" ET could significantly contribute to the catalytic activity observed for the full-length construct.

Interfacial Electron Transfer. In typical cases, forward and backward CV scans did not superimpose well (e.g., Figure 3b), which can be attributed to the reversible reductive inactivation described for NiR[11] (Scheme S1 in Supporting Information) and/or to a limiting mass transport.[8,10] Under conditions where these factors appeared less important (e.g., narrow scan ranges, low surface coverages), the voltammograms were reversible and independent of the scan rate between 10 and 100 mV/s (Figure S4 in Supporting Information), the latter scan rate corresponding to the maximum rate that still allowed for an accurate evaluation of the shape of the catalytic wave against the capacitive background. The reversibility implies that interfacial electron transfer (i.e., ET between Paz and the electrode) is faster than the rate-limiting step in the system.[8,10]

At reducing potentials below the sigmoidal (Nernstian) part of the catalytic wave, the catalytic current kept on increasing linearly with potential, which pertained down to at least −0.2 V (not shown). This is indicative of a distribution in electron-transfer rates between Paz and the electrode.[53,54] The experimental voltammograms are well fit by the equation derived for this situation[53] adapted to a one-electron process:[11]

$$\frac{\mathrm{d}i}{\mathrm{d}E} = -\frac{i_{\lim}}{\beta d_R}\frac{F}{2RT}\frac{1 + 2u\left(\upsilon^2 + \upsilon^4 + \frac{k_t}{k_0^{\max}}\upsilon^3\right) - \upsilon^4}{\left(1 + \upsilon^2 + \frac{k_t}{k_0^{\max}}\right)(1 + \upsilon^2)^2} \qquad (2)$$

with

$$u = \ln\left(\frac{1 + \upsilon^2 + \frac{k_t}{k_0^{\max}}\upsilon}{\frac{k_t}{k_0^{\max}}\upsilon}\right)$$

$$\upsilon = \exp\left(\frac{F}{2RT}(E - E_M)\right)$$

Here, di/dE is the first derivative of the catalytic wave at given potential, i_{lim} is the limiting catalytic current, β is the decay constant for electron transfer (a parameter indicating the effectiveness of the protein in mediating ET),[54] d_R is a range of distances between the electrode and the redox center, k_t is the catalytic turnover rate of the system, and k_0^{max} is the rate of electron transfer when Paz is optimally oriented on the electrode.

(53) Leger, C.; Jones, A. K.; Albracht, S. P. J.; Armstrong, F. A. *J. Phys. Chem. B* **2002**, *106* (50), 13058–13063.
(54) Jeuken, L. J. C. *Biochim. Biophys. Acta, Bioenerg.* **2003**, *1604* (2), 67–76.

For the voltammogram shown in Figure 3a, the fit yielded the following parameters: $k_t/k_0^{max} = 0.002$, $E_M = 0.243$ V, $i_{lim}/\beta d_R = 13$ nA for both scan directions. The low value of k_t/k_0^{max} shows that ET between the electrode and optimally oriented Paz is much faster than the turnover rate of the assembly.

Midpoint Potentials. In the case of fast interfacial ET between the electrode and Paz, the midpoint potential of the catalytic wave (E_M) occurs close to the lowest midpoint-potential of the sites participating in the redox pre-equilibrium preceding the rate-limiting step (see Note S1 in Supporting Information). In the current case, the rate-limiting step could either be the electron transfer between Paz and NiR (this includes the formation of the Paz/NiR complex, the ET step, and the dissociation of the complex) or the catalytic conversion of substrate. Thus, in case of a limiting ET between Paz and NiR, the E_M would be centered around the midpoint potential of the Paz T1 site, while in case of a rate-limiting catalytic step it would be centered around that of the Nir T1 (or T2) site. For the studied system, the E_M was always observed around 240 mV, which is within error of the E_M previously reported for the catalysis of isolated NiR at this pH,[11] but ~40 mV lower than the E^0 measured for Paz in solution using a MHX modified Au electrode (Figure 2). This would suggest, therefore, that NiR catalysis is rate-limiting. At present it cannot be excluded, however, that the midpoint potential of the Paz T1 site decreased as a result of its immobilization using negatively charged DNA.[36] For the current Paz/Nir system, a direct assessment of the redox potentials of the DNA-immobilized Paz and NiR Cu sites was precluded by the low surface coverages of the construct: no voltammetric features associated with the Paz and/or NiR copper sites stood out clearly from of the capacitive background in the absence of the nitrite substrate, either using electrodes assembled with the Paz component alone or with both the Paz and NiR components.

Ionic Strength Dependence of Catalysis. In an attempt to obtain further information about the rate-limiting step, the ionic strength (I) dependence of the catalytic rate of a fully assembled electrode was studied using CV. A remarkable increase of the catalytic current with increasing I was detected (Figure 6a). The first derivative di/dE of representative experimental voltammograms (Figure 6b) could be accurately fit to eq 2 in all cases, yielding values for $i_{lim}/\beta d_R$, E_M, and k_t/k_0^{max} at each I. The E_M did not significantly vary with the ionic strength (with an average of 242 ± 3 mV), indicating that the rate-limiting step does not change. The value for k_t/k_0^{max} was trending toward lower values at higher ionic strengths, varying between 0.007 and 0.004, indicating a decrease in the rate of catalytic turnover and/or an increase in the interfacial electron-transfer rate with I, although this trend was on the limit of significance (Figure S5 in Supporting Information). The low values obtained for k_t/k_0^{max} indicate that interfacial electron transfer is always much faster than the rate of catalysis over the range of I evaluated. The values for $i_{lim}/\beta d_R$ followed the trend observed for the i_{cat} measured at 0 V (not shown).

The large increase in i_{cat} with the ionic strength indicates that electrostatic interactions limit the turnover rate of the system, which points toward a rate-limiting electron transfer between Paz and NiR. An increase in I might diminish electrostatic interactions between Paz and/or NiR with the negatively charged anchor DNA, thereby preventing the system from getting locked in an unproductive state. This seems unlikely, however, considering that both proteins are negatively charged at the experimental pH of 6.8 (the isoelectric point of Paz and NiR are 6.4 and 5.3, respectively). This is in line with the observation

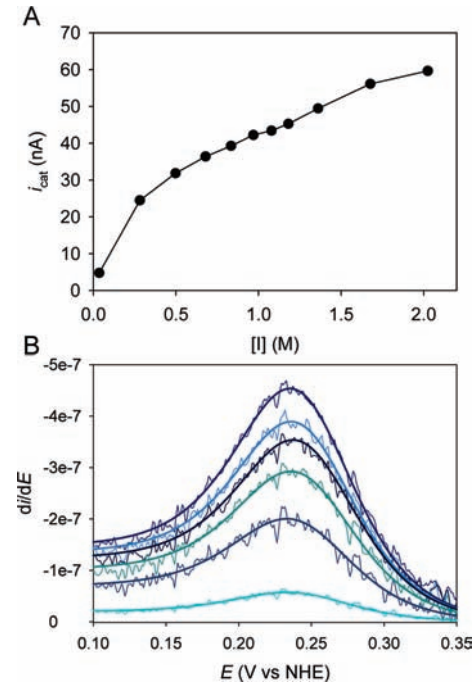

Figure 6. Ionic strength dependence of the CV of a fully assembled electrode. (a) The catalytic current measured at 150 mV versus I. (b) First derivative of representative background-subtracted voltammograms in the reductive scan direction at different values of I (0.04, 0.28. 0.50, 1.20, 1.36, and 1.68 M). The similar noise pattern in the data derives from the voltammogram used for the background correction.

that the catalytic current did not increase upon the addition of 10 mM Mg^{2+}, which compensates the negative charge of DNA, to the solution.[55] A more likely cause for the increase in i_{cat} is related to the sizable local concentration of Paz and NiR in the immobilized construct and the stability of the Paz/NiR complex. If it is assumed, for simplicity, that a NiR or Paz molecule may occupy a volume of a half-sphere with a radius on the order of 5−15 nm (the latter range corresponding to the approximate dimensions of the construct), the local protein concentration is between 0.2 and 6 mM. Such a concentration is higher than the solution K_d of 0.1 mM determined for the Paz/NiR complex at pH 6.5 and 0.04 M ionic strength,[31] thus predicting that the major fraction of Paz and NiR molecules are in complex under these conditions (this ignores the possible effects of the protein confinement on the K_d of the Paz/NiR complex).

Several studies have shown that the association of Paz and NiR is electrostatically driven where negative residues on the surface of NiR interact with positive charges distributed around the Paz electron-transfer patch.[31,56,57] A typical feature of such complexes is that the association rate k_{on} greatly diminishes with higher ionic strengths because of the screening of the charges involved in the intermolecular recognition,[58] whereas the dissociation rate k_{off} is much less effected, thus causing a net increase in the K_d ($= k_{off}/k_{on}$). In the current case, an increase in K_d would free Paz from the Paz/NiR complex, thereby making it available to interact with the electrode and causing a net

(55) MacKerell, A. D. *J. Phys. Chem. B* **1997**, *101* (4), 646–650.
(56) Kukimoto, M.; Nishiyama, M.; Ohnuki, T.; Turley, S.; Adman, E. T.; Horinouchi, S.; Beppu, T. *Protein Eng.* **1995**, *8* (2), 153–158.
(57) Kukimoto, M.; Nishiyama, M.; Tanokura, M.; Adman, E. T.; Horinouchi, S. *J. Biol. Chem.* **1996**, *271* (23), 13680–13683.
(58) Schreiber, G.; Fersht, A. R. *Nature Structural Biology* **1996**, *3* (5), 427–431.

enhancement of the catalytic efficiency. The progressive weakening of the Paz/NiR complex with increasing *I* has been previously invoked to explain a strong decrease in activity observed in a NiR activity assay using micromolar amounts of reduced Paz as the electron donor.[32] In the latter case, a factor of 5 decrease in activity was seen between 0.08 and 0.68 M ionic strength, which corresponds well to the 5-fold increase of i_{cat} over the same region of *I* in the current case. The effects of are opposite in both cases because the destabilization of the complex in the solution assay limits the flow of electrons to the NiR enzyme (the association of Paz and NiR is rate-limiting and becomes slower with higher *I*), while it would increase electron flow in the Paz/NiR construct by increasing the rate of Paz reduction at the electrode (more free Paz at higher *I*). The results predict that higher intermolecular ET rates could be attained at lower ionic strengths by weakening the Paz/NiR interaction, for example by the engineering of surface residues on Paz and/or NiR that are involved in the complex formation.[57]

Estimation of the Fraction of Electrochemically Active Construct. The fraction of electrochemically active construct on the surface can be estimated using the relation $\Gamma_{act} = i_{cat}/FAk_t$ in which Γ_{act} is the density of catalytically active construct (in mol/cm^2), *F* is the Faraday constant, *A* is the electrode area, and k_t is the turnover rate. At the optimal density of 1.5×10^{12} anchor molecules/cm^2 (2.5 pmol/cm^2), the catalytic current measured at 0 V, 1 mM NO_2^-, and 0.5 M ionic strength is 0.20 μA. This corresponds to 0.46 uA when the enzyme is fully saturated with NO_2^- as calculated using eq 1 and the experimental kinetic parameters (see above and Figure 4a). Furthermore, i_{cat} at 2 M ionic strength is at least double the i_{cat} measured at 0.5 M ionic strength (see Figure 6a), leading to an i_{cat} of at least 0.92 μA. If it is assumed that the turnover rate of the system is limited by catalysis by the NiR enzyme ($k_{cat} = 500$ s^{-1}), the density of active molecules can be calculated as 3.6×10^{11} molecules/cm^2. This suggests, therefore, that >24% of immobilized construct is electrochemically active (i.e., $> 4 \times 10^{11}$ active molecules/cm^2), which favorably compares with the reported density of electrochemically addressable NiR molecules absorbed on pyrolytic graphite (0.6×10^{11} molecules/cm^2).[11] The estimated percentage reflects a lower limit because of the following reasons: (1) The i_{cat} measured at 0 V was used for the calculation, whereas the limiting i_{cat} could not be determined due to the linear increase of i_{cat} at low potentials. (2) The maximum in i_{cat} is not yet reached at 2 M ionic strength. (3) It was assumed that NiR catalysis is rate-limiting, while the experimental data are consistent with a limiting electron transfer between Paz and NiR, implying a slower turnover rate.

Concluding Remarks

In summary, DNA-directed immobilization has been exploited to electrically contact a pair of interacting redox proteins to a SAM-modified gold electrode. All collected data is in agreement with the mechanism in Figure 1d in which Paz functions as an electron relay between the electrode and the NiR enzyme. Thus, despite being anchored to the surface, the proteins appear to maintain the mobility necessary to achieve ET between Paz and the electrode, as well as between Paz and NiR. The catalytic activity of the construct is consistent with reported data for NiR catalysis, showing that the enzyme remains functionally unperturbed by the immobilization. The rate of electron transfer from the electrode to the Paz component appears faster than the catalytic turnover rate of the assembly, corroborating the view that protein mobility on the electrode can help in establishing rapid interfacial electron-transfer kinetics.[28] This mobility would allow the protein to sample many orientations, thereby mimicking the dynamic ET processes in nature. The strong ionic strength dependence of the catalytic current indicates that the system reports not only on the interfacial electron-transfer kinetics and enzymatic catalysis, but also on the interaction between Paz and NiR. This provides clear perspectives for the use of DDI-based systems in the study of protein−protein interactions and biological electron transfer.

The combined results demonstrate that DDI permits the programming of intermolecular associations between multiple biological molecules to generate novel functions, in the current case to contact a "difficult" enzyme to an electrode surface. The immobilization becomes independent from the (surface) properties of the enzyme, contrasting conventional methods that often require a case-to-case optimization of the enzyme and/or the electrode surface. Hundreds of different redox enzymes are supplied with oxidizing or reducing equivalents by small electron-transfer proteins that have been proven suitable for electrochemical interfacing, suggesting that the strategy described here could be applicable to many other enzymes that do not readily interface with an electrode and/or denature when directly immobilized.

Although the methodology has been illustrated for a two-component system, it would also be applicable to single enzymes that are electrochemically well-behaved in solution but not when statically coupled to an electrode surface. Constructing more complex assemblies, containing a multitude of interacting redox proteins (or other electrochemically active components) immobilized on (branched) DNA templates, holds promise for future applications. The miniaturization of enzyme-modified electrodes to nanoscopic dimensions, where they potentially provide single molecule sensitivities, is rapidly advancing.[9,29,59] This, combined with the recent progress in DNA patterning and microarray technologies, suggests that the DDI-based method may also find uses in the development of lab-on-a-chip devices containing arrays of different DNA−protein modified microelectrodes.

Acknowledgment. This work was supported by a VENI grant from The Netherlands Organization for Scientific Research (NWO-CW). The author thanks Dr. A. Impagliazzo for supplying the structure of the Nir/Paz complex, Dr. M. Vlasie for supplying purified NiR and Paz, and Dr. H. Wijma for sharing his experience regarding the NiR enzyme and for supplying Scheme S1. Dr. H. A. Heering and Prof. T.J. Aartsma are acknowledged for helpful discussions. I thank Prof. Dr. G. W. Canters for his help during the writing stages of this manuscript and for his continuing support.

Supporting Information Available: Isotherm of the binding of SH-DNA$_{NP}$ to Au. DNase I induced disappearance of catalytic signal. Catalysis of the assembly in reverse orientation. Scan-rate dependence of the catalytic signal. Ionic strength dependence of k_t/k_0^{max}. Electrochemical setup. Catalytic mechanism of NiR. Apparent midpoint potential of the catalytic wave. This material is available free of charge via the Internet at http://pubs.acs.org.

JA101515Y

(59) Lemay, S. G.; van den Broek, D. M.; Storm, A. J.; Krapf, D.; Smeets, R. M.; Heering, H. A.; Dekker, C. *Anal. Chem.* **2005**, *77* (6), 1911–1915.